DOI: 10.13009/EUCASS2017-175

Experimental investigation of SLD impact phenomena

P. Berthoumieu, B. Déjean
ONERA – The French Aerospace Lab, F-31055, Toulouse, France

Abstract

The necessity of enhancing existing simulation tools to predict accurately the ice accretion cause by SLD is obvious [1]. This paper proposes an experimental approach of large droplet impact study in non-icing conditions but in high speed conditions. After a description of the experimental setup three different aspect of impact are proposed – Impact visualization in order to determine impact regime and limits – Reemitted droplets characterization (size and velocity) in case of splashing – Deposition rate of droplets on the wall for various conditions.

1. Introduction

Although the drops impact on walls has already been the subject of numerous studies in the past [2, 3], which have allowed a certain level of understanding, the physics of the impact requires further investigations to complete this knowledge. Indeed, good understanding and good modelling of the impact of drops is a prerequisite for the simulation of icing phenomena related to the impact of SLD (Supercooled Large Droplets).
The majority of the past experimental studies emphasize the number of Weber ratio between the aerodynamic forces and cohesive forces. In order to vary this number, the diameter is generally used. It is not evident that a drop of 10 µm impacting a wall at 100 m/s has the same behavior as a drop of 1 mm at 10 m/s, even they have the same number of Weber.
The objective of this work is to play on the drop impact velocity, without changing their diameter, in order to obtain values of the Weber number raised in relation to the reality encountered in the aeronautical world. In this study we tried to solve three delicate problems:

- Accelerate the drops without breaking them
- Observe the impact of small objects moving at high velocity
- Propose techniques for quantitative impact characterization.

All the presented work was done in the frame of the French research program PHYSICE funded by DGAC and dedicated to icing physics.

2. Experimental setup

The first part of the work consisted in designing and implementing a device to accelerate water droplets in order to reproduce the realistic conditions for drop / wall collisions.
The chosen solution is to inject calibrated drops into an air flow to accelerate them. This experiment is a first step before proceeding tests that should be conducted in a large-droplet freezing tunnel to improve our understanding of the SLD behavior in icing conditions. The difficulty of this kind of wind tunnel is to be able to accelerate the drops without breaking them. There are numerous studies in the literature on the secondary fragmentation of drops by aerodynamic effects. The number of Weber is used to define the limit below which a drop maintains its cohesion.

$$We = \frac{\rho_{air}(U_{air} - U_{drop})^2 d_{drop}}{\sigma}$$

This value is fixed between 10 and 12 according to the authors, beyond this value occurs the rupture of the drop.
The objective is to accelerate drops from the injection velocity to the highest possible speed.
The droplet generator used for this work is able to deliver droplets with an identical size and spacing in a large range of diameters (Figure 1). Droplets are generated by applying a mechanical excitation on a small diameter liquid jet. The excitation is given by a piezoelectric ceramic driven by a function generator. The droplet size is directly linked

DOI: 10.13009/EUCASS2017-175

to the excitation frequency imposed at the ceramic, the diameter of the liquid jet which is fixed by the exit hole of the injector, and the liquid flow rate. The relationships shown below are used to determine optimal injection conditions:

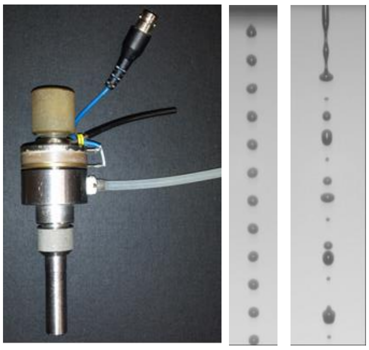

Figure 1 – Droplet generator and stream
(left: injector, center: with excitation, right: without)

Droplet diameter: $D_d = \sqrt[3]{\frac{6Q}{\pi f}}$

Droplet spacing: $S_d = \frac{V_d}{f}$

Optimal excitation wavelength given by Rayleigh theory: $\lambda_{opt} = 4{,}51.\Phi_0$

Optimal frequency $f_{opt} = 0{,}198.\frac{V_{inj}}{\Phi_0}$

When the optimal frequency is used, the droplet diameter is $D_d = 1{,}9.\Phi_0$

The excitation frequency should be adapted to the liquid flow rate and the injector hole, so as to obtain a monosized droplets stream. The diameter of the drops depends essentially on the diameter of the orifice and can be slightly modified by varying the excitation frequency. The initial velocity of the drop depends essentially on the flow rate and therefore on the injection pressure. The use of this injector makes it possible to generate drops with a speed varying between 5 and 10 m/s by modulating the injection pressure of the water. However, this assembly does not make it possible to obtain the drops at the desired speed which is around 80 m/s. This is why it will be necessary to accelerate the drops.
To do this, the drops are introduced into an airflow whose velocity increases gradually in order to avoid the breakup of the drops by the aerodynamic forces. The injector is therefore placed at the entrance of a long convergent. A tool for calculating the velocity of the drops in a flow has been developed in order to optimize the geometry of the convergent. This tool is based on a balance of forces on the drop, friction and gravity, to obtain the drop velocity and the differential with the surrounding air velocity and thus be able to calculate a Weber number at any point. This numerical simulation made possible to find a geometry that is simple to realize and more efficient.

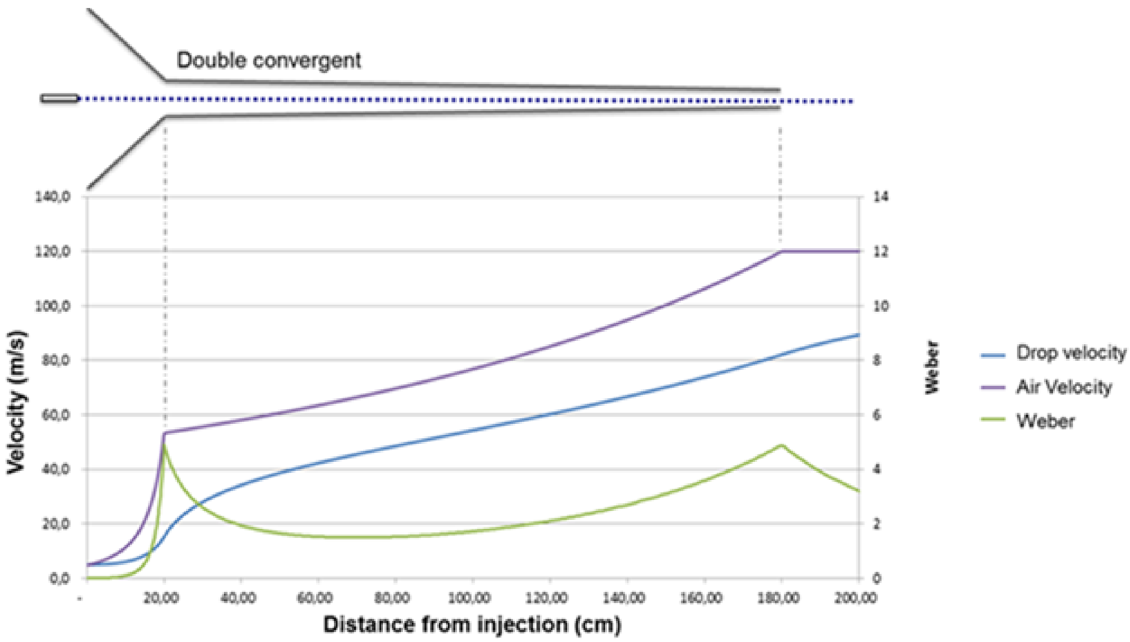

Figure 2 - 200 µm diameter droplet speed up.

They are two successively arranged linear convergents. The first convergent rapidly accelerates the air in the vicinity of the injector what allows the drops to be moved apart as quickly as possible and thus limit the coalescence. The second convergent accelerates the air more gradually and reduces the speed difference between the drops and the carrier flow. Figure 2 shows the result of the simulation for a drop of 200 µm in the double convergent. For an air

DOI: 10.13009/EUCASS2017-175

velocity at the output of 120 m/s, the drop reaches a final velocity of 85 m/s without ever fragmenting since the Weber number does not exceed 5, the rupture of the drop occurring for values between 10 and 12.

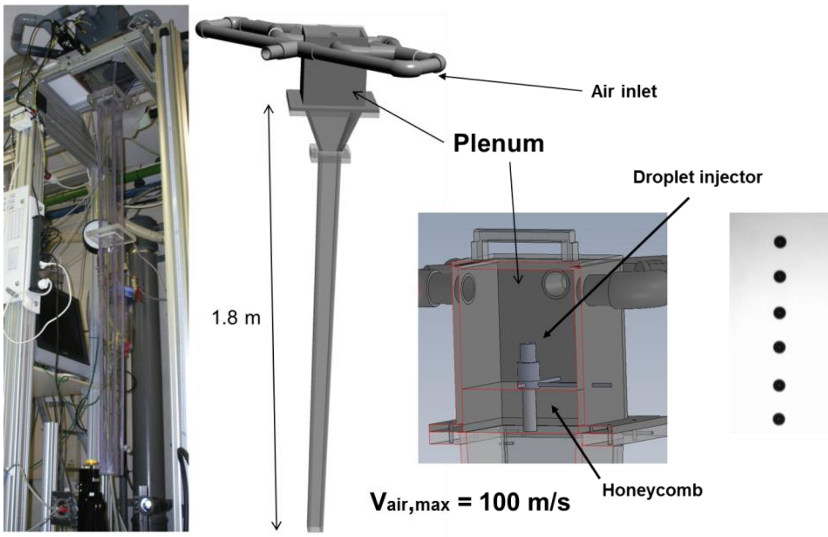

Figure 3 – Particle acceleration system

However, the speed equilibrium between the air and the drop is not obtained. To reach it, it would be imperative to increase the length of the convergent. To achieve this equilibrium, it would take a length greater than 5 m. This was not possible and the convergent was dimensioned according to the constraints of the room, the air supply closest to the ceiling and the test area at 50 cm from the ground.
Previous tests [6] carried out in a wind tunnel have shown the necessity of having a vertical installation to overcome the gravity, which modifies the trajectory of the drops as a function of their mass and of the speed of the carrier air. This assembly is supplied with air by the compressed air network of the laboratory, high pressure compressors produce air up to 80 bar, stored in a 16 m^3 tank and then expanded for use in the vicinity of 10 bar. The flow rate used is controlled by a Coriolis control valve and flowmeter system to guarantee a constant speed in the convergent.
A plenum chamber was created upstream of the convergent. It allows to house the monodisperse injector and also to limit the level of turbulence at the input of the convergent. In order to reduce its speed, the air enters through the four faces of the plenum chamber. A grid creating a slight pressure drop is placed in the flow just above a honeycomb to break the large turbulent structures and homogenize the upstream flow (Figure 3).

For a given injector hole, impacting droplet sizes may vary with surrounding air flow.

Measurements

Several means of phenomenon characterization have been implemented. Qualitative means in a first step and subsequently tools enabling quantitative characterization of the impact have been used. It concerns the estimation of deposition rate on the wall and, for the re-emitted part, measurement of secondary drops size and velocity.
Phenomena observation is an essential step in their characterization; moreover this phase helps to better understand the phenomenon and to understand how it unfolds. The majority of the visualizations of the drop impact are realized by shadowing, the camera and the light source being placed on each side of the object to be observed. Under these conditions the drops appear dark on a light background.
The drops are animated by a high velocity and it is necessary to freeze them to avoid the blur induced by their motion, so it is necessary to have a very short shutter time. In general, the target field is a few millimeters, each pixel of the camera sees an area that varies between 5 and 10 µm of sides. In order not to have a fuzzy effect of the movement of the particles, the displacement of the object in the field must be less than one pixel. For a speed of 10 m/s this corresponds to a shutter time of between 0.5 and 1 µs. As we aim at higher speeds, it will be necessary to achieve shutter speeds of a few tens of nanoseconds. Only few cameras allow this. So we worked on lighting with very short flashes. For this purpose, we used light-emitting diode systems, which provide flashes with a duration varying between 0.2 and 1 µs or a laser diode system with a flash time of up to 20 ns. Then there is a need of synchronization between the image taken and the presence of a drop in the field.

DOI: 10.13009/EUCASS2017-175

The probability that a drop passes through the field of view of the camera is extremely low, it is necessary to find a system for detecting the passage of drops in the field of the camera. The simple detection of the passage of a drop in a laser beam is not sufficient. It is necessary to detect the drop just before it enters the field of the camera, which represents a few millimeters long and a few tenths of a millimeter thick. To do this, we have developed a system inspired by the principle of LDA systems, a laser beam illuminates the area of interest and a photosensitive element collects the light scattered by the drops crossing the zone. The received signal is filtered and shaped to be then sent to the camera, which retransmits it to the illumination system for imaging with a delay to let the particle enter in the field of view. Thanks to this technique, all images carry information.

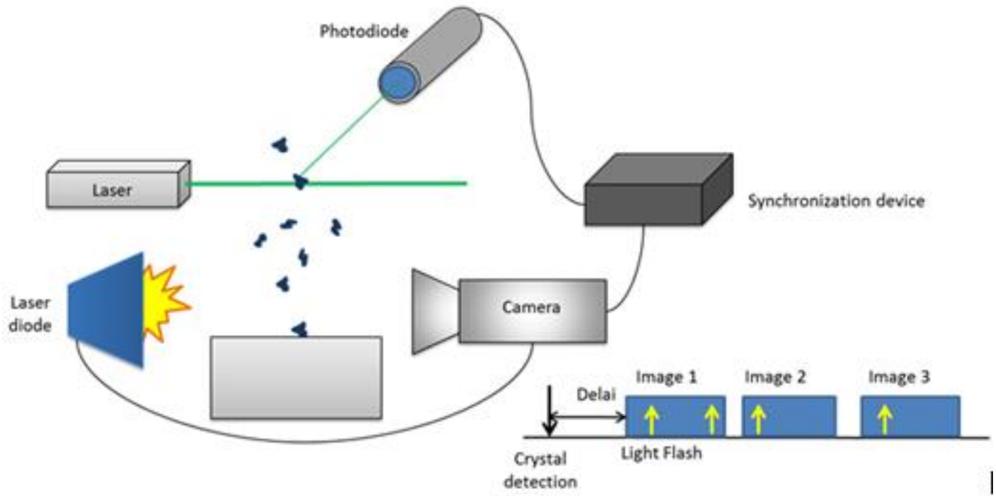

Figure 4 – Particle detection system

A 180 mm macro lens SIGMA was used to obtain a sufficient magnification to observe ice crystals and their impact. The field of view was 6.5 x 4.5 mm with a pixel size of 5 µm.
The chosen solution for droplet impact observation is the use of a PIV type camera which allows taking three successive images with intervals that can go down to 1.5 µs. The camera, JAI AD 131 GE, offers a very good resolution compared to high speed video systems (1,296 x 966 pixels of 3.75 µm sides). The rate of the image triplets is 30 frames per second. By decreasing the inter-frame time, a very high-speed camera can be simulated, up to 600 000 im/s but limited to 3 images.
In order to make the best use of this small number of images, the first image is devoted to obtaining the characteristics of the incident particle; two flashes illuminate the particles at two moments before impact to be able to measure its size and velocity.
The lighting system was a Cavilux laser diode that could generate very intense flashes with a short duration. The light was focused to send the maximum of energy into the camera.

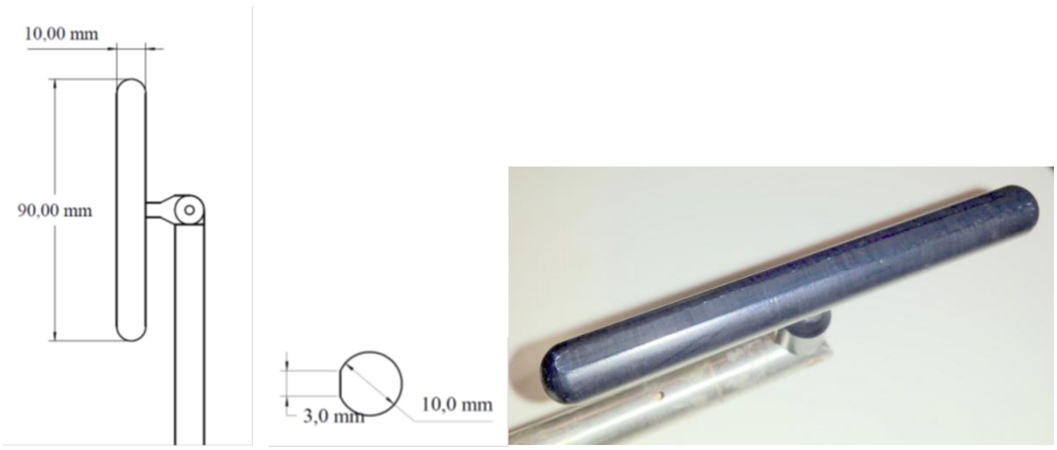

Figure 5 – Test wall for visualization and PDA measurement

DOI: 10.13009/EUCASS2017-175

For the visualization of the behavior of the drops during the impact, we used a wall machined from a cylindrical bar of 10 mm diameter on which a flat part was machined (Figure 5). This element is made of anodized aluminum to give it a constant surface finish over time. An articulation allows changing its inclination and therefore the angle of impact of the drops. The covered range is from 0 to 90°.
Visualizations were made for driving air speeds ranging from 40 m/s to 100 m/s and for three impact angles of 90°, 60° and 30°. The images proposed below correspond to drops from an orifice of 150 µm therefore a size varying from 300 to 450 µm. The intervals between images have been adapted as a function of the driving air velocity in order to best describe the dynamics of the observed phenomenon. The images taken by the camera cover a field 3.7 mm high by 4.8 mm wide.
The following images correspond to a normal impact for driving speeds of 40 and 80 m/s, they were chosen arbitrarily in the sequences taken, the only criterion was based on the diameter of the incident drop in the vicinity of 260 µm. On the first images, with a relatively low impact velocity, the phenomenon of corolla formation is still relatively visible, and atomization results from the fragmentation of the liquid film forming the corolla. When the speed of impact increases this phenomenon disappear, the atomization is done earlier and closer to the wall, the created drops become smaller.

We = 2 000 - Dg = 258 µm – Vg = 24 m/s

We = 9 300 - Dg = 259 µm – Vg = 51 m/s

Figure 6 – Droplet normal impact for two velocities

When the impact angle changes the morphology of the phenomenon remains at first similar. In order to obtain the images of Figure 7, the wall was inclined by 30° (impact angle 60°), and in order to follow the phenomenon as well as possible, the camera was also rotated by 30°. In the images the drops arrive obliquely but in reality their fall is always vertical and aligned with the air flow. Secondary drops appear to be carried away more rapidly by the air flow which goes from right to left.

DOI: 10.13009/EUCASS2017-175

We = 1 550 - Dg = 258 µm – Vg = 24 m/s

We = 6 800 - Dg = 255 µm – Vg = 51 m/s

Figure 7 – Impact with an angle of 60° for two velocities

We = 400 - Dg = 252 µm – Vg = 22 m/s

We = 8 900 - Dg = 255 µm – Vg = 50 m/s

Figure 8 – Impact with an angle of 30° for two velocities

When the inclination of the wall passes to 60° (impact angle 30°), the impacts are more grazing and an asymmetry of the formed corolla can be noticed and one finds films of liquid, which detach themselves from the wall as during normal impact with low number of Weber. The secondary drops are very quickly swept away by the air flow.
This setup is useful for high impact angles, when the angle become lower than 10° the droplet detection system is not precise enough and it is very difficult to observe impacts because of an inaccuracy in the droplets localization. To observe precisely the impact phenomena it is necessary to use a high magnification lens that is to say a small field of view. If there is an error in the droplet detection, the impact may occurs out of the field of view (Figure 9 left sketch).

DOI: 10.13009/EUCASS2017-175

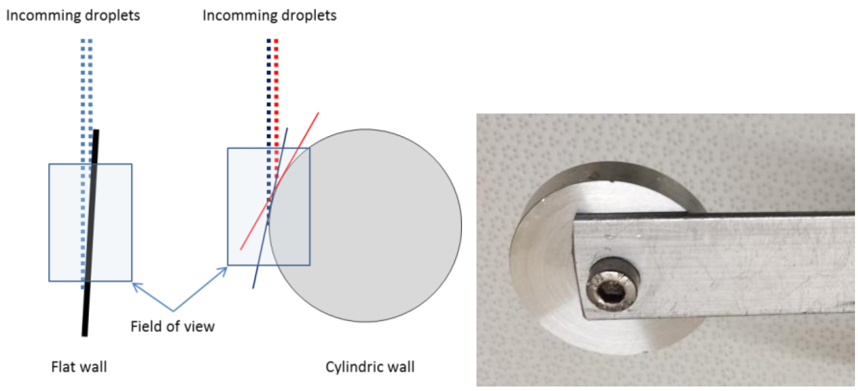

Figure 9 – Small impact angle setup

The use of a cylindrical wall avoids this problem. Each localization corresponds to a different impact angle so instead of a fixed angle per experiment we have a continuous description of various impact angles in the same test.

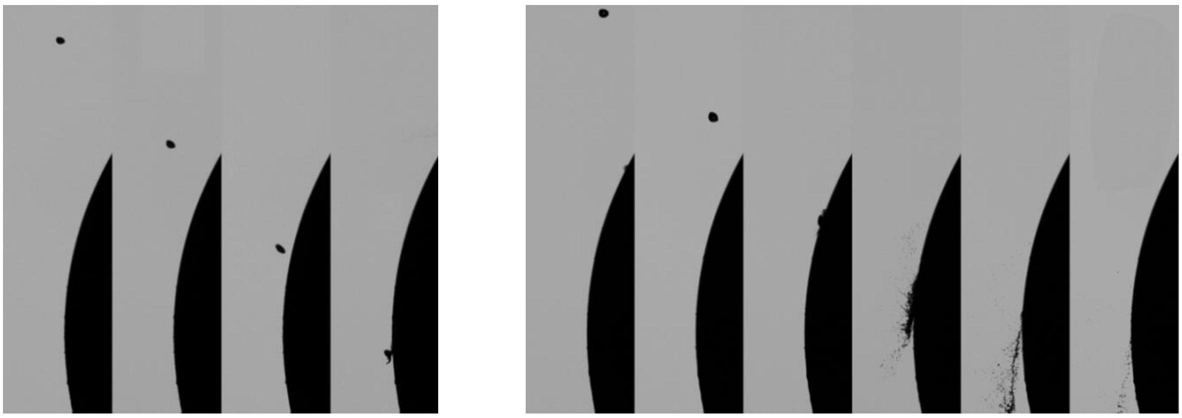

Rebound *Splashing*

Figure 10 – High speed visualization for low droplet velocities

The first tests were conducted with a high speed camera. To obtain time-resolved sequences, it is necessary to decrease image size. Therefore, these sequences (Figure 10) are useful for understanding but they are not spatially resolved to use them to measure carefully drop size and velocity. Once again, we use the PIV camera with sets of three images.
The first image with a double exposure is processed to extract droplet diameter, velocity and trajectory to determine precisely the impact location on the cylinder and then calculate impact angle (Figure 11).

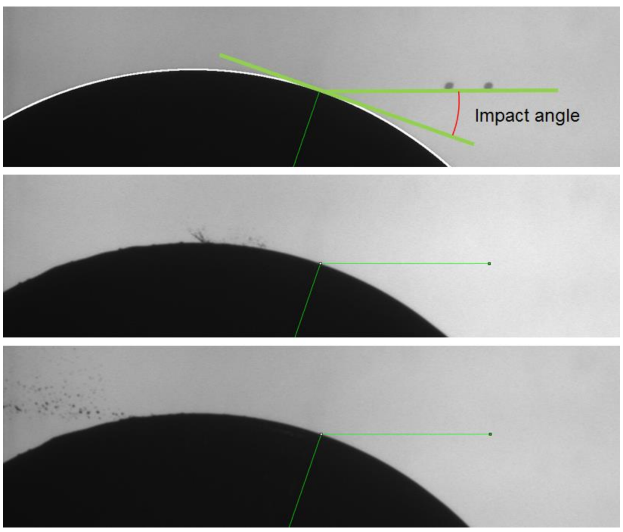

<u>Double exposition image :</u> t0 and t0 + 30 µs

- Droplet detection
- Size and spacing measurement
- Impact angle calculation

<u>Impact :</u> t0 + 210 µs

Determination of the impact régime (splash or rebound)

<u>After impact :</u> t0 + 390 µs

Figure 11 – Impact image analysis (D=380 µm U= 58 m/s)

DOI: 10.13009/EUCASS2017-175

To complete the impact visualization a set of experiment has been conducted to determine the impact regimes limits. Parametric tests have been conducted:

- Three different air velocities (40, 60 and 80 m/s)
- Two droplets sizes (400 µm and 250 µm)
- Two different wall materials (aluminum and Teflon)

More than 9000 set of three images have been analyzed to determine if it exist a limit angle value for rebound and its sensitivity to droplet size or velocity. For each run images are processed to calculate the impact angle and the operator determine the impact regime. Results are plotted as the probability of rebound as a function of impact angle.

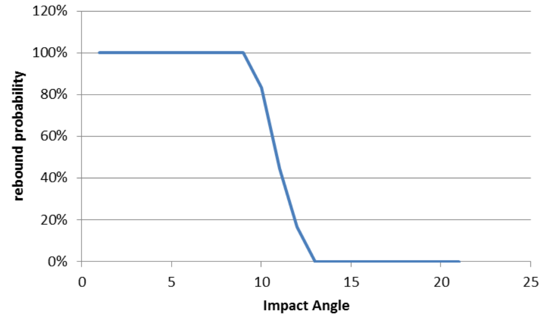

Figure 12 – Rebound probability as a function of impact angle (D = 400 µm U = 57 m/s)

In this plot (Figure 12) it can be see that rebound is always visible when impact angle is below 9° and after there is a transition in which rebound and splash are present together and above 13° splash was only detected. In order to compare the effect of size, velocity and wall material such plots have been superposed.

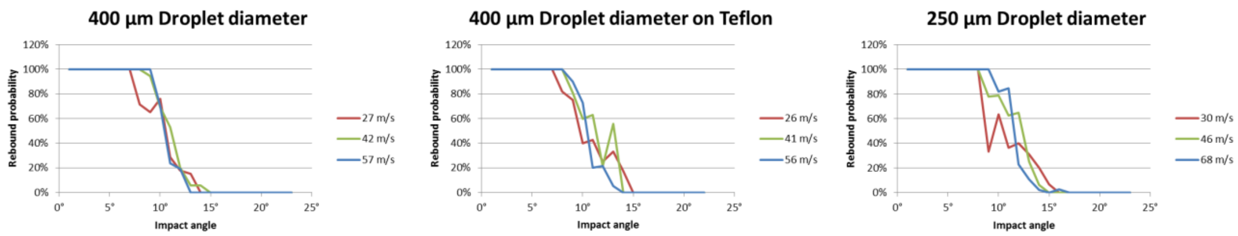

Figure 13 – Rebound probability as a function of impact angle for various tests

The beginning of the transition starts for all the tested configurations close to 8 or 9° impact angle. For low droplet velocities (red plots in Figure 13) the transition begins for small angles and spreads to higher angles. For higher velocities the transition between rebound and deposition is sharpen.

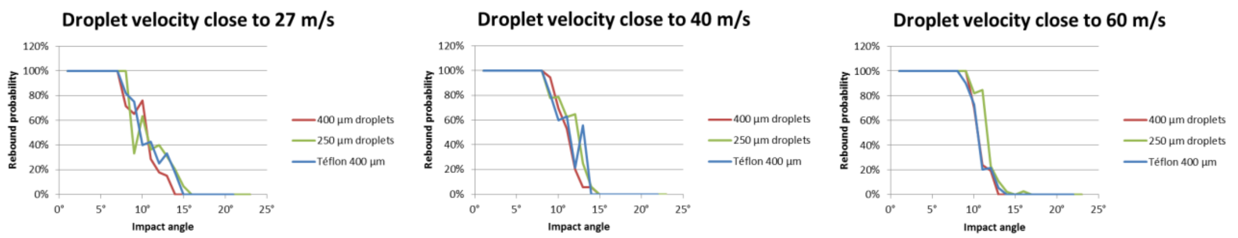

Figure 14 – Rebound probability as a function of impact angle for various droplet velocities

Another way to compare these data is to group them by equivalent incoming velocities (Figure 14) to highlight a possible influence of other parameters. The conducted tests do not permit to validate droplet size influence or wall material. On the whole, we can consider that for SLD droplets the transition occurs between 9° to 15° independently of droplet velocity and size.

DOI: 10.13009/EUCASS2017-175

Deposition rate

The next step of this work is, when there is splashing, to determine the amount of liquid that remains on the wall after the impact of the drop. This value is of prime importance for the icing simulation codes, in fact a bad consideration of this value will lead to erroneous accretion shapes. This quantity is very difficult to measure; there are no means of obtaining precisely this value. A solution is proposed here to estimate this quantity. It consists of trying to recover the liquid, which settles on the wall and then weigh it.
The assembly consists of a flat plate on which the drops are impacted. This plate has dimensions greater than the output section of the convergent. It is supposed to receive the impact of all the incident drops.

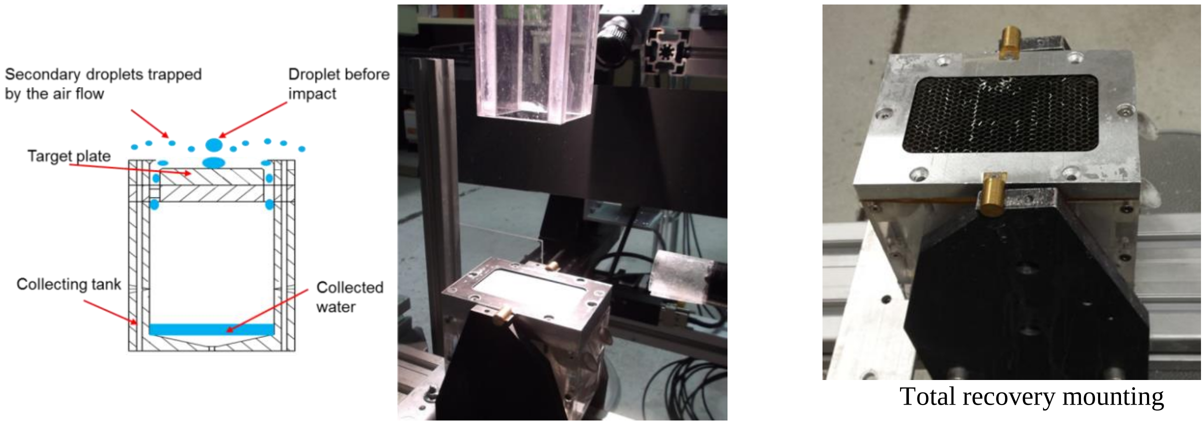

Total recovery mounting

Figure 15 – Deposition rate measurement setup.

The portion of the drops which settles on the wall flows towards the edges and is then recovered in a reservoir situated under the plate, the majority of the secondary drops being carried away by the flow. This plate has a planar rectangular shape in order to be able to tilt it and to study the influence of the impact angle on the deposition rate.
This plate is exposed to droplet impacts for several minutes and the recovered liquid is then weighed and compared to the amount of incident liquid to determine the average deposition rate.
The implementation of this method was more difficult than expected because the measures are very sensitive to external conditions. In the first place it is necessary to evaluate with precision the quantity of liquid that actually impacts the wall. Despite the precautions taken the airflow around the drops is quite disturbed and disperses the drops in the convergent and some of them will even impact the walls of the vein and do not reach the target. Another source of loss of mass is the evaporation of the drops during their transport and that of the liquid deposit on the surface of the plate. The use of the humidifier made it possible to limit this evaporation without being able to avoid it. Indeed it is practically impossible to work in totally saturated air at the risk of generating condensation and thus have uncontrolled liquid water inputs. The tests will therefore be carried out with a regulated relative humidity around 70%.
The first tests showed the need to have a very strict and rigorous procedure to be able to compare the results.
A test sequence involves exposing the plate to drops for several different impact angles. Typically for a given operating point, air velocity and droplet size, the test sequence begins with the recovery of all the liquid that impacts the wall. To do this, the wall is replaced with a honeycomb like that the liquid flows towards the storage tank (Figure 15).
At the end of this measurement we have the quantity of liquid that really impacts the wall. The following tests correspond to the various angles of impact, from 90° to 10°. Each point of measurement gives rise to the weighing of the recovered mass. The sequence ends with a new total liquid recovery point in order to control the stability of the installation. The evolution of the recovered masses is monitored continuously so as to duplicate any outliers. Throughout the duration of each test point, flow, temperature and humidity measurements are acquired continuously, and a pre-impact image of the droplets is used to monitor size and velocity characteristics. The following table shows the droplet characteristics before impacting the wall.

Air velocity / Hole diameter	40 m/s		60 m/s		80 m/s	
	Mean diameter	Droplet velocity	Mean diameter	Droplet velocity	Mean diameter	Droplet velocity
70 µm	215 µm	30 m/s	195 µm	46 m/s		
100 µm	255 µm	29 m/s	325 µm	42 m/s	305 µm	56 m/s
150 µm	460 µm	25 m/s	430 µm	39 m/s	370 µm	52 m/s

Droplets characteristics

DOI: 10.13009/EUCASS2017-175

The results obtained for each test condition are plotted on Figure 16 the various curves are identified with the test conditions, air velocity and droplet generator hole. A plateau is visible for impact angles greater than 50° the deposition rate can be consider like constant. For lower angles a decrease is observed. This is in agreement with the observations carried out in the first part of the document. When a droplet impinges the wall with a law impact angle it tears on the surface and a large amount of liquid is carried away by the flow so the deposition is low.

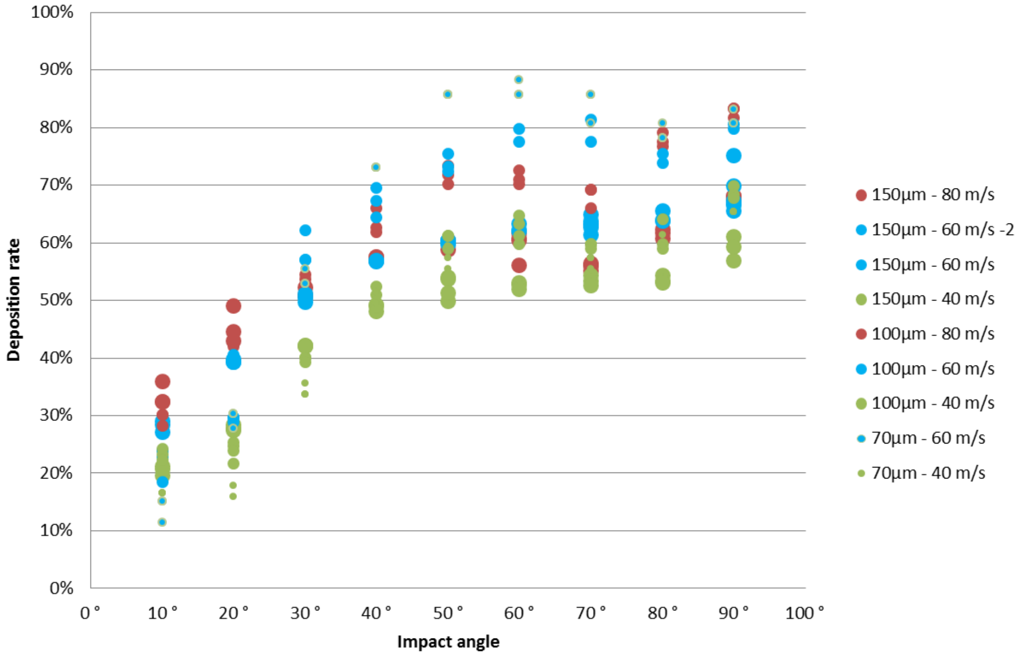

Figure 16 – Deposition rate measurement results.

The lowest deposition rate is also observed for the lowest impact angle that is in agreement with the previous observation. For this value, only a low percentage of droplets splashes on the wall, the others rebound. Some other representations of these data have been tested, function of Weber number (Figure 17) or the impact K parameter, which give the same result.

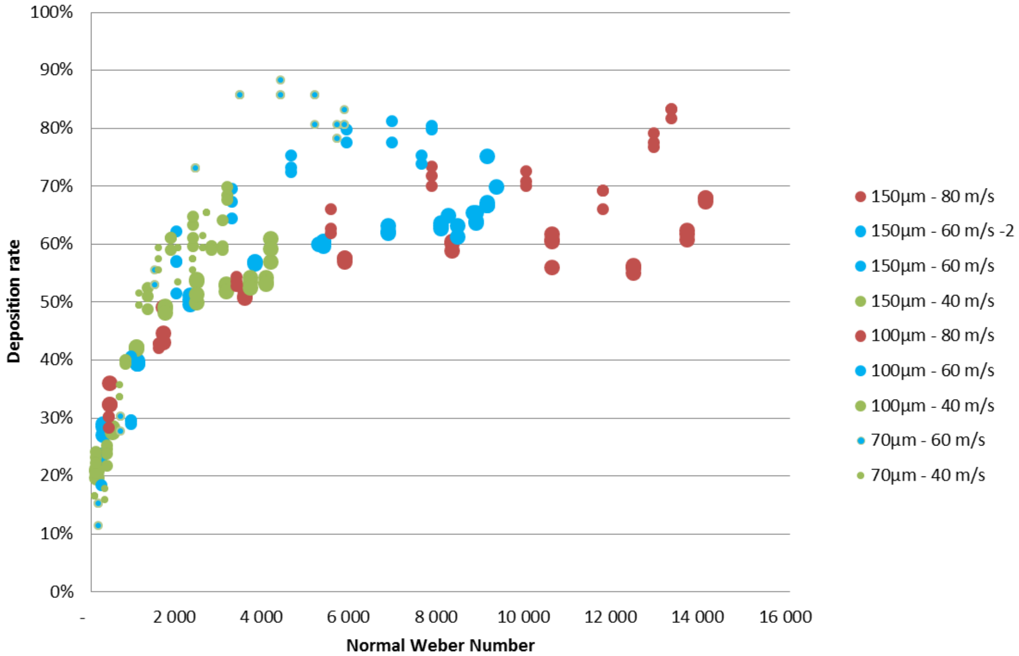

Figure 17 – Deposition rate measurement results as a function of Weber number

DOI: 10.13009/EUCASS2017-175

For the lowest values of Weber number, the measures are well correlated but when We is greater than 3000 a very large dispersion is visible.

Droplet re-emission characterization

The next phase consists in characterizing the re-emitted drops after impact on the wall. To do this we used a Phase Doppler Analyzer. This non-intrusive system makes it possible to measure the size and two components of the velocity of spherical particles passing through the measurement volume. The measurement volume is the result of the intersection of two laser beams; it is ovoid in shape, 0.3 mm in diameter and about 4 mm in length.
The system used is a PDA from Dantec, it works with two 300 mW solid lasers (532 nm and 671 nm), which allow the exploration of relatively dense sprays. For the configuration used, the emission focal length is equal to 500 mm and that of reception is equal to 400 mm. The angle of observation is equal to 30°. Under these conditions, the measuring range extends to 542 μm.
The measuring volume is positioned 1 mm above the wall. This distance corresponds to a compromise between the probability of having drops passing through the measurement volume and a sufficient distance not to be in the corolla due to the impact. Thus, for an air flow at 60 m/s, the average number of drops passing through the measuring volume located 1 mm from the surface is close to 90 drops per second and falls to 3 drops per second at 4 mm from the wall. The duration of acquisition is limited to 5 minutes per test point or 40 000 drops acquired, in order to have values representative of the phenomenon observed. The measurements were carried out for air velocities varying between 20 and 100 m/s making it possible to accelerate the drops more or less. Different sizes of incident drops were produced by changing the injector hole (50, 100 and 150 μm) in order to scan a range of Weber number as large as possible. Finally, these impacts were performed for three angles of impact 0° -30° and 60°. In the end more than 40 configurations were analyzed.

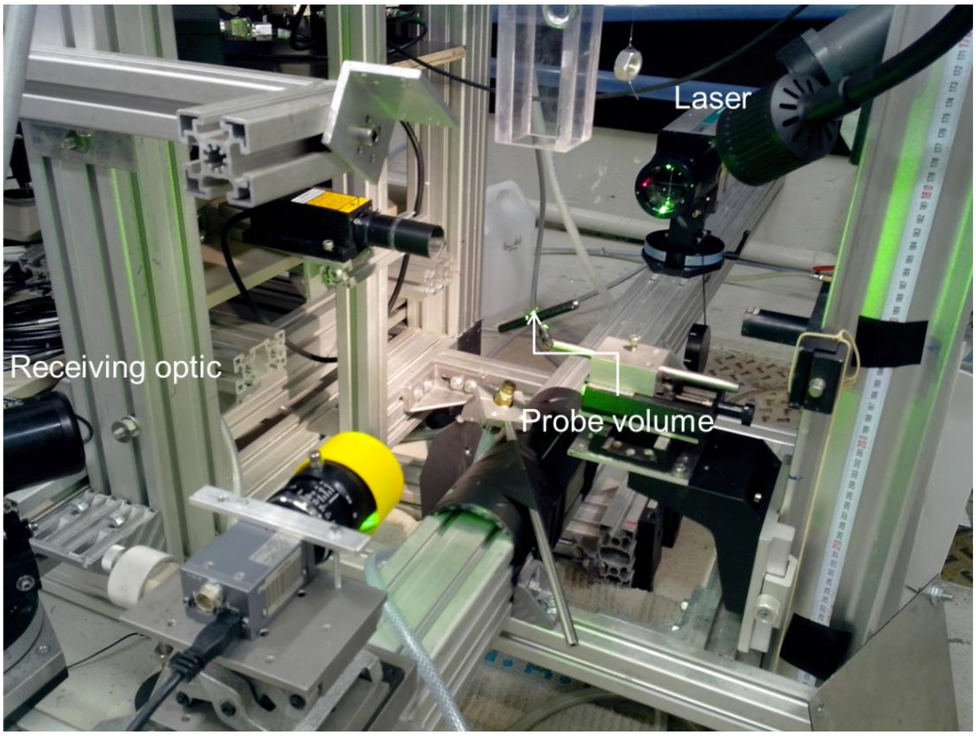

Figure 18 – Montage du granulomètre phase doppler

During measurement all the drops passing through the measuring volume are taken into account whatever their trajectory. It can be consider two kinds of droplets. The one which have just been ejected from the wall and have a trajectory which moves them away from the wall, and the others which fall towards the wall and in this case they have a trajectory that will make them impact again. In order to keep only the first one, drops leaving the wall, a procedure for selecting drops has been developed. An export of the raw data of each measured drop: diameter and two components of the velocity is realized. The velocity vector is then calculated and according to its orientation with respect to the wall, the drop is taken into account or rejected. Only the drops leaving the wall are taken into account in the following results.

DOI: 10.13009/EUCASS2017-175

This sorting affects very little the average sizes of the drops but has a great importance on the speed under consideration.
For each measurement point histograms of the size distribution of the drops measured after the impact are plotted. In the Figure 21, it is possible to observe an example of results concerning normal impact of incident droplets with a diameter varying between 350 and 400 µm. The mean velocity of these drops is given by the surrounding air flow and it varies from 12 and 68 m/s from air varying from 20 to 100 m/s.

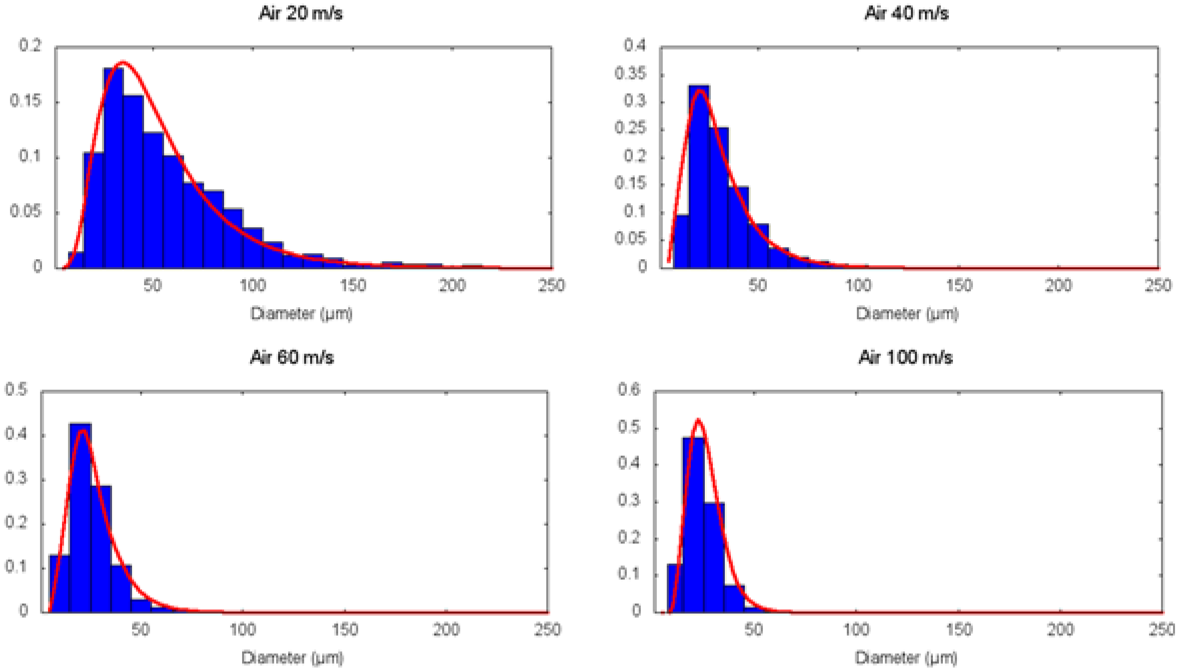

Figure 19 – Drop size repartition after normal impact (orifice 150 µm)

Depending on the droplet impact velocities, these histogram narrows towards the small ones, this is in perfect agreement with the observations described before. It is also possible to obtain a good fitting of these histograms with a Log Normal distribution law. A similar evolution is also visible with a lower impact angle.

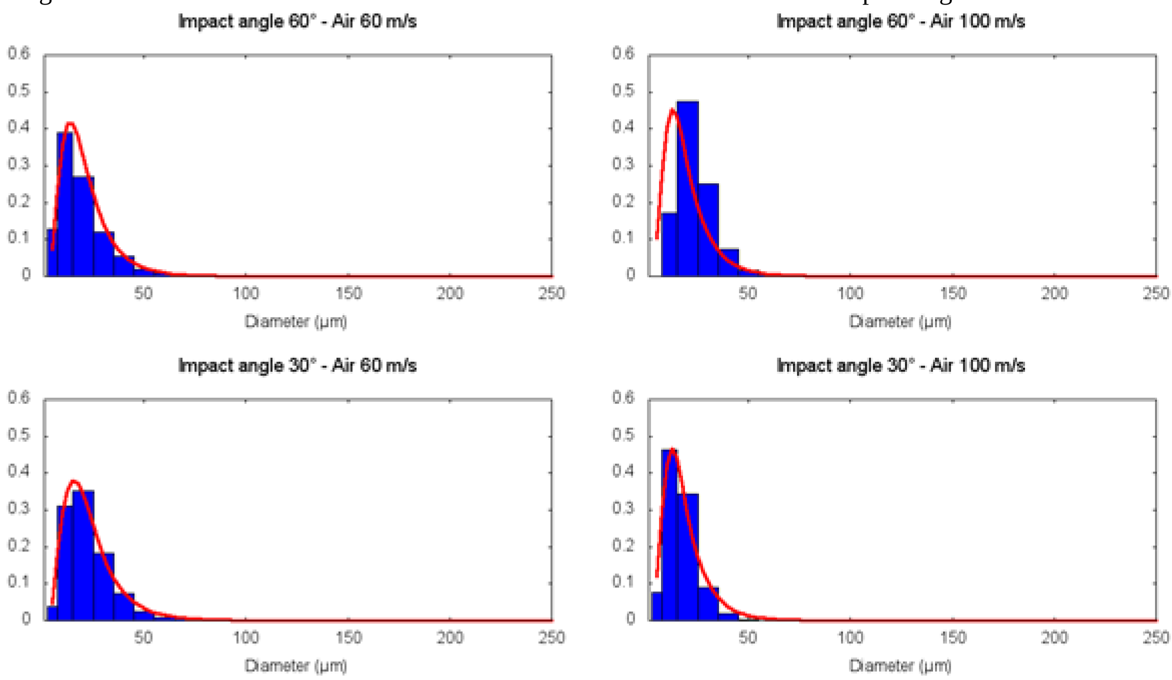

Figure 20 – Drop size repartition after 60° and 30° impact angle (orifice 150 µm)

In each case the same law is applied for the Log Normal fitting curve (in red).

DOI: 10.13009/EUCASS2017-175

The results of all of our tests can be summarized by the following two graphs (Figure 20) where the mean diameter and diameter of Sauter (D32) are shown.

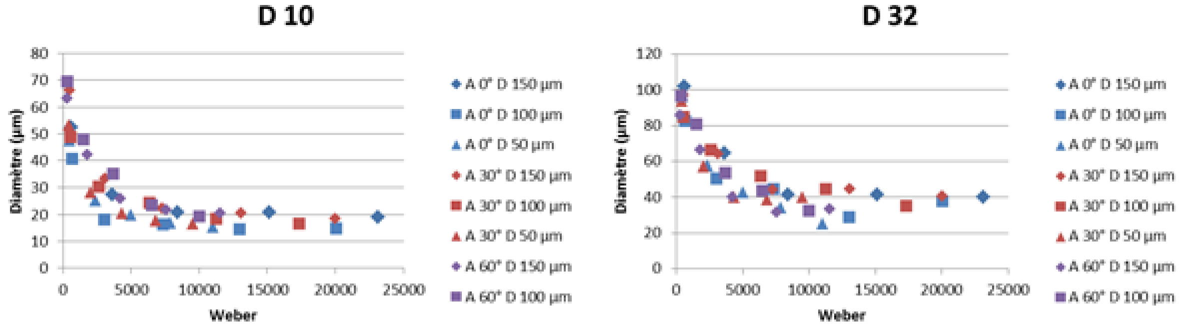

Figure 21 – Diameter evolution after impact

These graphs gather the measurements made for various incident droplet sizes ranging from 150 µm to 450 µm and velocities from 15 m/s to 80 m/s. The different symbols allow identifying the test conditions, impact angle and diameter of the injection orifice of the drops. Whatever the test conditions, the diameter of the re-emitted drops follows a regular progression as a function of the Weber number calculated on the incident normal velocity.

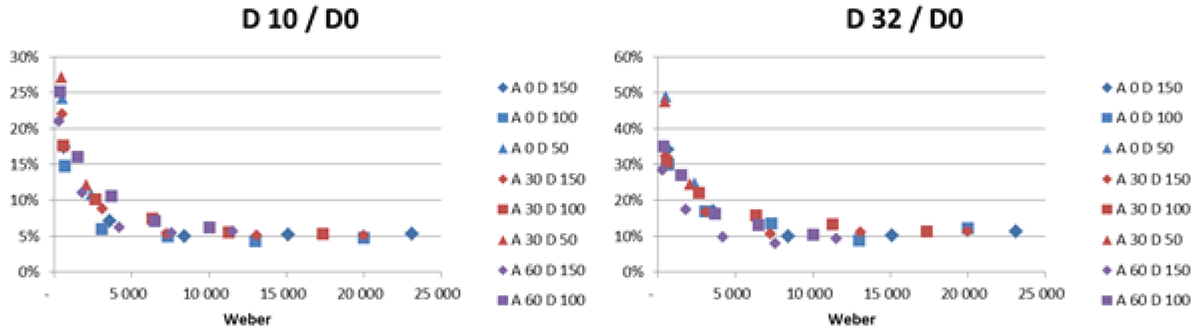

Figure 22 – Diameter evolution after impact

The normalization of these diameters with respect to the diameter of the incident drops makes it possible to reduce the dispersion of the measurements somewhat.

Conclusion

In this study a new test medium was created and implemented to study the impact of high-speed drops. This means, admittedly limited in terms of maximum possible speed, nevertheless enabled us to obtain an unpublished database on this subject.

This experiment proved difficult to operate so much the parameters influencing the impact of drops are numerous. The droplet acceleration system has proved to be effective, although it provides some dispersion of the drops in the area of impact, the use of a conical convergent would surely improve the flow by eliminating the effects corner. The first experiments of recovery have shown the very great importance of the control of the humidity of the air used to accelerate the drops, which necessitated the design and the realization of an assembly allowing to better control this hygrometry.

The visualizations have informed us about the dynamics of the impact which begins with forms of corollas very regular for the low speeds to lead to a total bursting of the drop when the speed is important. They also show the dependence of the size of the re-drops with the speed of impact.

The particle size measurements of the reemitted drops show a regular decrease in diameter when the Weber number increases. This is in perfect agreement with our observations.

A weighing technique was used to estimate the deposition rate. This technique is very difficult to implement and requires relatively long experience, but the results obtained are encouraging.

DOI: 10.13009/EUCASS2017-175

Furthermore, work needs to be done to extend this measurement at speeds even greater than those achieved in this study, but this will require the fabrication of a longer convergent. It would be interesting to continue in this way to complete the basis of giving and making comparisons with numerical simulations.

References

[1] Giuseppe Mingione, Emiliano Iuliano, Didier Guffond, Cameron Tropea "EXTICE: EXTreme Icing Environement" *SAE 2011 International Conference on Aircraft and Engine Icing and Ground Deicing, June 2011*.

[2] Mundo Chr, Sommerfeld M, Tropea C, "Droplet-Wall Collisions: Experimental Studies of The Deformation And Breakup" *Process, Int. J. Multiphase Flow*, Vol 21, No.2, p151-173, 1995.

[3] Hammond, D., Quero, M., Ivey,P., Purvis,R., McGregor, O., Tan, J., "Analysis And Experimental Aspects Of The Impact Of Supercooled Water Droplets Into Thin Water Films," *AIAA-2005-077, AIAA conference, Reno, 2005*.

[4] Luxford, G., Hammond, D., Ivey, P., "Modelling, Imaging and Measurement of Distortion, Drag and Break-up of Aircraft-icing Droplets", *AIAA-2005-71, AIAA conference, Reno, 2005*.

[5] S.C. Tan, M. Papadakis, D. Miller, T. Bencic, P. Tate, M.C. Laun "Experimental Study of Large Droplet Splashing and Breakup" *AIAA-2007-904, , AIAA conference, Reno, 2007*

[6] P. Berthoumieu, "Experimental Study of Supercooled Large Droplets Impact in an Icing Wind Tunnel." *AIAA 2012-3130, , AIAA conference, New Orléans, 2012*